COMPUTATIONAL FLUID DYNAMIC SIMULATION OF NON-NEWTONIAN TWO-PHASE FLUID FLOW THROUGH A CHANNEL WITH A CAVITY

by

Mehdi AHMADI* and Ayoob KHOSRAVI FARSANI

Department of Mechanical Engineering, Islamic Azad University,
Shahrekord Branch, Shahrekord, Iran

Original scientific paper
https://doi.org/10.2298/TSCI180102151A

In this paper, the numerical solution of non-Newtonian two-phase fluid-flow through a channel with a cavity was studied. Carreau-Yasuda non-Newtonian model which represents well the dependence of stress on shear rate was used and the effect of n index of the model and the effect of input Reynolds on the attribution of flow were considered. Governing equations were discretized using the finite volume method on staggered grid and the form of allocating flow parameters on staggered grid is based on marker and cell method. The QUICK scheme is employed for the convection terms in the momentum equations, also the convection term is discretized by using the hybrid upwind-central scheme. In order to increase the accuracy of making discrete, second order Van Leer accuracy method was used. For mixed solution of velocity-pressure field SIMPLEC algorithm was used and for pressure correction equation iteratively line-by-line TDMA solution procedure and the strongly implicit procedure was used. As the results show, by increasing Reynolds number, the time of sweeping the non-Newtonian fluid inside the cavity decreases, the velocity of Newtonian fluid increases and the pressure decreases. In the second section, by increasing n index, the velocity increases and the volume fraction of non-Newtonian fluid after cavity increases and by increasing velocity, the pressure decreases. Also changes in the velocity, pressure and volume fraction of fluids inside the channel and cavity are more sensible to changing the Reynolds number instead of changing n index.

Key words: *volume of fluid method, two-phase flow, Carreau-Yasuda model, numerical simulation, finite volume method, non-Newtonian fluid*

Introduction

The difference between both classes of fluids can be observed in a variety of situations. However, as far as we know, the studies on gas and non-Newtonian liquid two-phase flows across singularities in mini-channel are still limited. Non-Newtonian fluids, such as paint, milk, toothpaste, animal blood*, etc.* are ubiquitous in nature, and they are often encountered in many industries, like in chemical engineering, plastic manufacturing, wire and fiber coating, transpiration cooling, heat pipes, biological fluids, gaseous diffusion, drilling muds, biochemical engineering, food processing, oil exploration, and medical engineering [1, 2]. Particularly in industrial applications, non-Newtonian fluids are of great interest, since many used fluids,

* Corresponding author, e-mail: ahmadi.m@iaushk.ac.ir

lacquers or polymer solutions show non-Newtonian effects. So the viscoelastic fluid can enhance the displacement efficiency, which has been proved by lots of experimental results [3-5].

The Carreau [6] viscosity model is considered as an appropriate viscosity model to describe the rheology of the non-Newtonian liquid due to its capability to describe the zero-shear-rate and the infinity-shear-rate Newtonian viscosity limits. Payang *et al*. [7] and Bakht *et al*. [8] presented the calculation of viscoelastic flows of Oldroyd-B fluid. they used numerical method. In another research, Huang *et al.* [9] studied 2-D incompressible fluid-flow of shear cavity. Both in Euler frame and Lagrangian frame, were simulated by SPH, FPM, the original KGF-SPH and improved KGF-SPH. Xu *et al.* [10] applied a fractional flow model to describe a time-variant behavior of non-Newtonian substances. Freydier *et al.* [11] reported high resolution measurements of the velocity field within the front of free surface viscoplastic surges in an inclined channel.

Over the past decades, significant advances have been made in numerical modeling of two-phase flows. For examples, the two-fluid model [12, 13] and the discrete particle model [14, 15] were developed to simulate two-phase flows. The front-capturing method [16] and the front-tracking [17] methods, were developed to capture the free surfaces of multi-phase flows. The flows of two immiscible liquids are encountered in a diverse range of processes and equipment. An overview of these approaches is described in [18-22].

Despite the fact that a plethora of multi-phase flow models are available in the literature, the information regarding the simulation of two-phase with a non-Newtonian fluid on a channel with a cavity is quite limited. Also, despite of their importance, liquid-liquid-flows have not been explored to the same extent as gas-liquid-flows. In fact, gas-liquid systems represent a very particular extreme of two-fluid systems characterized by low-density ratio and low viscosity ratio. In liquid-liquid systems, the density difference between the phases is relatively low. However, the viscosity ratio encountered extends over a range of many orders of magnitude. In the present work, the numerical solution of non-Newtonian two-phase fluid-flow through a channel with cavity is studied. The input fluid in the channel is modeled as a Newtonian fluid and the liquid in the cavity is modeled as a non-Newtonian fluid. Carreau-Yasuda non-Newtonian model which represents well the dependence of stress on shear rate is used and the effect of *n* index of the model and the effect of input Reynolds on attribute of flow are considered. For the description of the interface, we employed the volume of fluid (VOF) method. Based on the velocity of input fluid we considered the flow laminar.

Modelling and simulation

Mathematical model

In this paper, non-Newtonian two-phase fluid-flow in a channel with cavity was studied as shown in fig. 1. The flow, was assumed isothermal and 2-D. The VOF method was used to investigate the flow of polymer solution discharged into the water from the cavity. The polymer solution is modeled as a non-Newtonian fluid, and the water is modeled as a Newtonian fluid. The Carreau [6] viscosity model is considered as an appropriate viscosity model to describe the rheology of the non-Newtonian liquid, due to its capability to describe the zero-shear-rate and the infinity-shear-rate Newtonian viscosity limits. The aim of this paper is to study the effect of changes in input Reynolds number by changing the input velocity and changes in

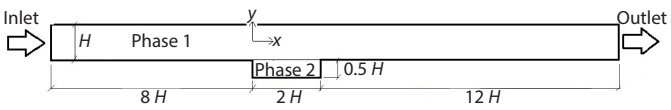

Figure 1. The geometry of problem

n index of Carreau-Yasuda model. Therefore, first, the flow field consist of non-dimensional velocity, pressure drop and then volume fraction of phases will be studied. To achieve this purpose in two-phase flow problems, mass fraction of two different phases in the flow field needs to be calculated. In the present study a VOF method is used. The volume fraction of a fluid is introduced as an additional variable in the governing equations.

The basic equations were discretized using the finite volume method (FVM). In the FVM, the computational domain is divided into a large number of control volumes. The primitive variables are defined at the center points of each control volume. Further information about FVM is explained in the literature [23-25]. The numerical solution of the question was conducted by SIMPLEC algorithm and computer programming was written by FORTRAN.

The equations of non-Newtonian two-phase fluid

Two-phase non-Newtonian flow field in a channel with cavity is derived by continuity, momentum and a model which describes viscosity of non-Newtonian fluid. Also we need an extra equation that describe interface of two-phases. The two-phase flow temperature is assumed to be constant at 300 K. We consider steady, incompressible and isothermal flow in a 2-D Cartesian co-ordinate system, x and y. The aforementioned equations can be expressed [26, 27]:

$$div\, u = 0 \tag{1}$$

$$\frac{\partial}{\partial t}(\rho u) + \rho(u\nabla)u = div\, \boldsymbol{S} - \nabla p \tag{2}$$

where ρ is the density, t – the time, u – the velocity, and $\boldsymbol{S}$ – the stress tensor that can be expressed:

$$\boldsymbol{S} = 2\mu(\dot{\gamma})\boldsymbol{D} \tag{3}$$

$$\boldsymbol{D} = \frac{1}{2}\left[\nabla \boldsymbol{u} + (\nabla \boldsymbol{u})^T\right] \tag{4}$$

$$\dot{\gamma} = \sqrt{2tr(\boldsymbol{D}^2)} \tag{5}$$

where $\boldsymbol{D}$ is deformation tensor and $\dot{\gamma}$ – shear rate. For the viscosity function, we recall the Carreau model [6]:

$$\mu(\dot{\gamma}) = \mu_\infty + (\mu_0 - \mu_\infty)\left[1 + (\lambda\dot{\gamma})^2\right]^{(n-1)/2} \tag{6}$$

where μ_0 is zero-shear-rate viscosity, μ_∞ – infinite-shear-rate viscosity, λ and n are constants which are determined by experimental investigations and characterize the used fluid.

The volume of fluid method

The VOF method, which originates from the idea of Hirt *et al.* [28], is a technique where the volume fraction of each phase in a cell is calculated. The major advantage of the VOF method is its conservative nature. A brief review of VOF method can be found in [29-32]. The VOF method can also be modified or coupled with other techniques to improve its ability in solving multi-phase flow problems [33-35]. The VOF function evolves according to the following advection equation:

$$\frac{\partial f}{\partial t} + \nabla(uf) - f\nabla u = 0 \tag{7}$$

where u denotes the velocity vector that can be found from solution of the flow field. The VOF function f has a value between 0 and 1. By solving eq. (1), the distribution of f is obtained. In a physical sense, eq. (1) implies mass conservation of one phase in the mixture. Numerically, eq. (1) is characterized as a hyperbolic or pure convection equation.

Boundary conditions

Generally, boundary conditions to solve the equations are as follows: no slip boundary conditions are assumed at the solid wall for velocity [36]:

$$u = 0, \quad v = 0, \quad \frac{\partial u}{\partial x} = 0, \quad \frac{\partial v}{\partial x} = 0, \quad \frac{\partial v}{\partial y} = 0 \tag{8}$$

The stress components at the wall are obtained by solving constitutive equations and by applying known velocity boundary conditions.

At the outlet the Neumann boundary conditions are imposed for the flow variables:

$$\frac{\partial u}{\partial x} = 0, \quad \frac{\partial v}{\partial x} = 0, \quad \frac{\partial \tau_{xx}}{\partial x} = 0, \quad \frac{\partial \tau_{yy}}{\partial x} = 0, \quad \frac{\partial \tau_{xy}}{\partial x} = 0 \tag{9}$$

Boundary values for pressure-correction equations are determined by considering velocity boundary conditions. At inlet we know velocity profile.

Solution procedure

Equations that have been already derived, can be used to calculate flow field parameters. To conduct calculations in this study, governing equations are discretized using finite volume method [37-39] on staggered mesh. The form of allocating flow parameters on staggered mesh are based on marker and cell method. The QUICK scheme is employed for the convection terms in the momentum equations. The convection term is discretized by using the hybrid upwind-central scheme. To increase the accuracy of making discrete, the second order Van Leer accuracy method is used [40]. For mixed solution of velocity-pressure field SIMPLEC [41] algorithm is used. For pressure correction equation iteratively line-by-line TDMA solution procedure and the strongly implicit procedure is used. To ensure the achievement of steady-state, the appropriate under-relaxation technique is used. Besides that, due to use of low Reynolds number model to solve the velocity field, it is required that a sufficient number of grid points in the near-wall boundary-layer. Special attention has thus been paid to the grid refinement, particularly for computing two-phase flow field. The solution process is reiterated until the maximum relative changes of flow variables, u, v, p, τ_{xx}, τ_{yy}, and τ_{xy}, are less then 10^{-6}.

Grid study

Grid refinement is one of the most important issues in non-Newtonian two-phase flow simulations. In order to acquire accurate results and capture realistic flow, especially near the walls and fluid phase boundaries that have considerable changes in some parameters. Also it is necessary to review the effect of varying the number of grid nodes on the flow parameters. For this purpose, the generalized Newtonian fluid-flow is used at Re = 500. As fig. 1 illustrates, the problem geometry consists of three sections; upstream of the cavity, the cavity, and downstream of the cavity represented by 1, 2, and 3, respectively. For different grids, different numbers of nodes are considered in the horizontal and vertical directions. For each section, the names of these four grids are G1, G2, G3, and G4, respectively. Grid specifications are shown in tab. 1.

Table 1. Number of nodes for different grids

Grid	Number of nodes section 1	Number of nodes section 2	Number of nodes section 3
G1	3600	2400	3600
G2	7200	4800	7200
G3	14400	9600	14400
G4	28800	19200	28800

Table 2. Values of relative errors of the longitudinal velocity at the center of the channel outlet at Re = 500 and n = 0.7-1

n	EG1	EG2	EG3
1	0.28	0.12	0.03
0.9	0.30	0.11	0.04
0.8	0.26	0.18	0.02
0.7	0.27	0.14	0.02

Table 3. The longitudinal velocity at the center of channel outlet for different Reynolds number

Re	200	500	1000	1500
u	1.499117	1.499125	1.499120	1.499120

Table 4. Comparison between the centerline velocities of parallel-plate channel for different n and Re = 500

	Present work	Analytical
n = 0.50	1.327	1.333
n = 1.00	1.495	1.500
n = 1.25	1.546	1.555

The uniform square grid G4 was considered as the reference mode. Given that the responses for this grid are precise, the responses for the coarser grid were compared with those of reference mode. The values of the relative errors of the longitudinal velocity at the center of channel outlet for generalized Newtonian fluid-flow at Re = 500 and n = 0.7-1 are shown for three grids in tab. 2. As seen in tab. 2, the difference between the values obtained using G3 and G4 is negligible. Thus, the uniform grid G3 is selected to run the program.

Validation

Numerical simulation of non-Newtonian fluid-flow in the desired geometry is done by grid G3. This grid is suitable in terms of both the accuracy and time of calculations. To investigate the performance of the computer code, the numerical results obtained are compared with analytical results at two state. In the first state as already mentioned, Carreau-Yasuda non-Newtonian model at n = 1 is turned into a simple Newtonian fluid. With regards to the assumption of the generalized flow at channel outlet, the maximum velocity at the center of channel is 1.5. The longitudinal velocity derived from the numerical solution at the center of channel outlet for different Reynolds values are shown in tab. 3. In the second section validate the computer code, computations are made in a smooth parallel plate channel and the results thereof are compared with available analytical solutions and experimental data. For n = 0.5, 1, 1.25, and Re = 500, a comparison of centerline velocity between this study and the analytical results [42] is shown in tab. 4. As illustrated, a good agreement is found.

Result and discussion

Non-Newtonian two-phase fluid-flow in a channel with a cavity

After the performance of computer code was ensured and appropriate grid was selected, different runs were conducted at different states. All calculations for water as Newtonian fluid and solution polymer as non-Newtonian fluid were conducted and constant geometry as fig. 1. Reynolds number varied between 500-1500. The rheological parameter, n, varied between

Table 5. Coefficients of Carreau-Yasuda model

ρ [kgm^{-3}]	n	λ [s]	μ_0 [Pa·s]	μ_∞ [Pa·s]
800	0.7-1	0.036	0.00345	0.056

0.7-1. In following sections, the effects of change in Reynolds number and rheological parameter, n, on the flow parameters were investigated. Coefficients of Carreau-Yasuda model are presented in tab. 5.

The effect of Reynolds number

In this section, we changed Reynolds number only. The geometrical specs were considered constant as shown in fig. 1. Also rheological parameter of non-Newtonian fluid, n, was considered constant as $n = 0.8$. Figure 2 indicates streamlines for different Reynolds numbers. Based on the distribution of the streamlines, it can be seen that by increasing Reynolds number, the central vortex moves up and downstream the cavity.

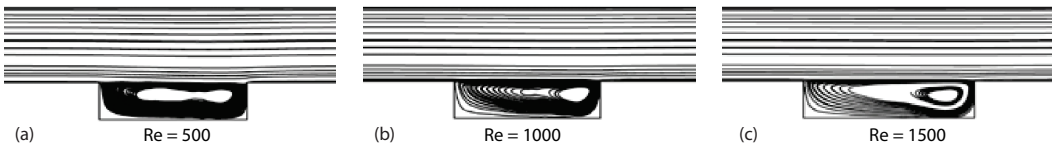

Figure 2. Streamlines for different Reynolds number and $n = 0.8$; (a) Re = 500, (b) Re = 1000, and (c) Re = 1500

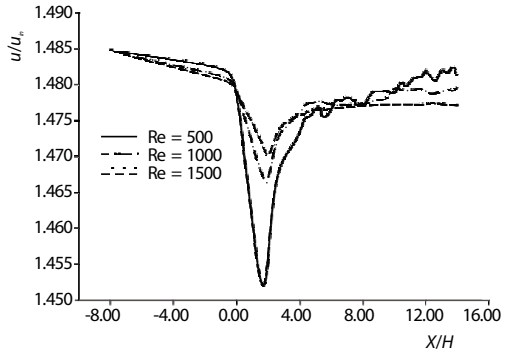

Figure 3. Velocity distribution at central line of channel for different Reynolds number and $y = 0$, $n = 0.8$

As illustrated in fig. 2 the bottom corners and parts of the near-wall regions of the cavity are not covered with the Newtonian fluid. However, by increasing Reynolds number, these areas become smaller, but not fully covered. This is due to the rheological nature of non-Newtonian fluids that show resistance to breaking up.

Figure 3 shows the longitudinal velocity of the Newtonian fluid at $y = 0$ from the channel inlet to the channel outlet for various Reynolds numbers. As shown in fig. 3, by decreasing the Reynolds number, the vertical velocity position moves upward, and the region with negative velocity in the cavity increases. When non-Newtonian fluid enters the channel it mixes with the Newtonian fluid and results in a two-phase flow.

As we can see in fig. 4 by increasing Reynolds number initially, the volume fraction of non-Newtonian fluid increases in the channel. Since the flow rate of the Newtonian fluid in channel is constant. As non-Newtonian fluid enters into the channel and decreasing the cross-sectional flow, the velocity of Newtonian fluid increases first, and then, due to the decrease in the flow rate of non-Newtonian fluid into the channel it reaches to steady-state.

Figure 5 shows the distribution of non-dimensional longitudinal pressure at the center of the channel. The linear pressure distribution of upstream and downstream cavities represents the flow developed before and after the cavity. In the cavity area due to the increased cross-section, the velocity decreases and the pressure increases. With regard to the results obtained in the case of pressure, increasing the Reynolds number decreases the pressure flux. The effect of the non-Newtonian fluid is due to the nature of its dilution.

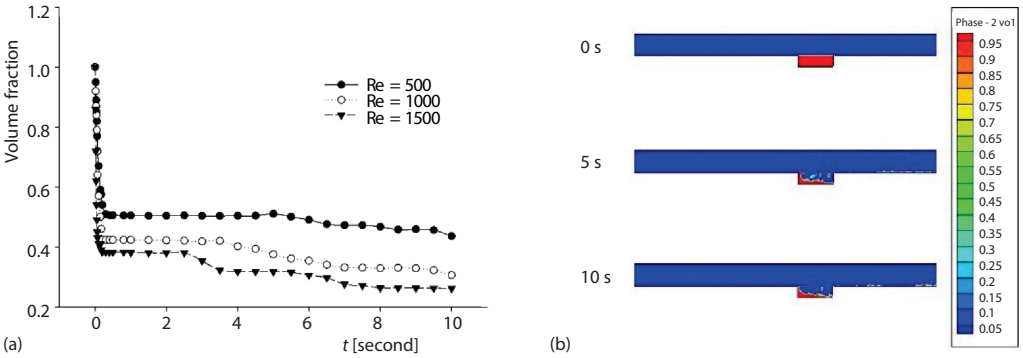

Figure 4. Volume fraction of non-Newtonian fluid in the cavity; (a) for different Reynolds number, n = 0.8, (b) Re = 1000, n = 0.8

The effect of rheological parameter

In this section, we changed rheological parameter, n, only. Geometrical specs were considered constant as shown in fig. 1, also Reynolds number was considered constant as Re = 1000. Figure 6 indicates streamlines for different rheological parameter, n. The rheological parameter, n, affects the viscosity and also affects the flow of non-Newtonian fluid and discharging process. Based on the distribution of the streamlines, it can be seen that as n incresses, the central vortex moves up and downstream the cavity.

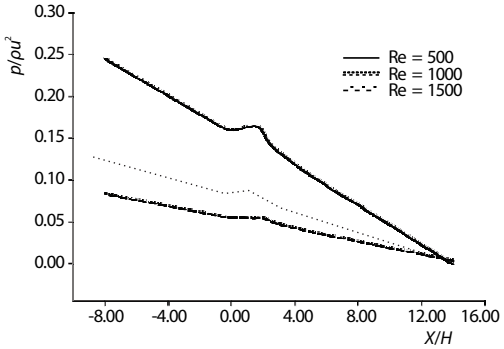

Figure 5. Distribution of longitudinal pressure at the center of the channel for different Reynolds number, n = 0.8

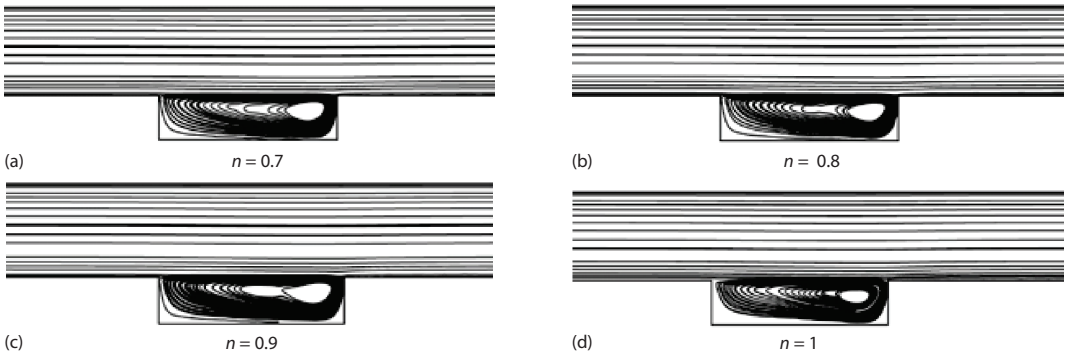

Figure 6. Streamlines for different n and Re = 1000; (a) n = 0,7, (b) n = 0.8, (c) n = 0.9, and (d) n = 1

As mentioned earlier, the effect of inertia on fluids with a higher n is higher, and so the fluid is moved upstream easily. In fig. 6, it can be seen that the elongation rate of the interface area that is caused by fluid displacement in cross-sectional area is higher for fluids with a higher n, and therefore, the mixing of the fluid is better and the discharge time is reduced as we can see in fig. 7. Downstream the cavity two-phase flow occurs and velocity increases, as we can see in fig. 8. The increase in velocity for fluid with higher n is higher.

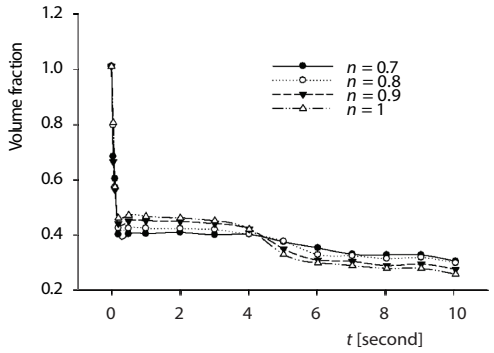

Figure 7. Volume fraction of non-Newtonian fluid in the cavity for different *n* and Re = 1000

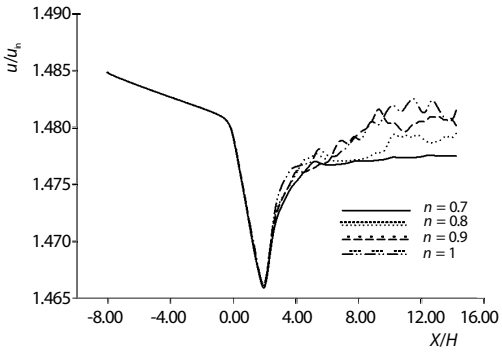

Figure 8. Velocity distribution at central line of channel for different *n* and *y* = 0, Re = 1000

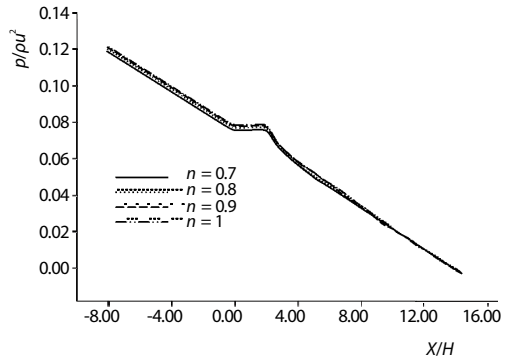

Figure 9. Distribution of longitudinal pressure at the center of the channel for different *n* and Re = 1000

With the increase in rheological parameter, *n*, the shear rate viscosity decreases and the flowing areas in the dead corners (at bottom of cavity) are enlarged markedly, thus the area with no flow becomes smaller significantly. Because of this reason sweep area and efficiency increase as *n* increases.

In the cavity area due to increased cross-section, the velocity decreases and the pressure increases. With regard to the results obtained in the case of pressure which are shown in fig. 9, increasing in *n*, raiseses the pressure flux. The effect of the non-Newtonian fluid is due to the nature of its dilution.

Conclusion

In this paper, non-Newtonian two-phase fluid-flow in a channel with cavity was studied. As streamlines show, by increasing Reynolds number the central vortex moves upstream and downstream the cavity. Also by increasing Reynolds number, the time of sweeping the non-Newtonian fluid inside the cavity decreases. Also the discharging time of the cavity reduces and the two-phase region downstream the cavity increases. Since the flow rate of the Newtonian fluid in channel is constant, as non-Newtonian fluid enters into the channel and the cross-sectional flow decreases, the velocity of Newtonian fluid increases and the pressure decreases. In the second section, by increasing rheological parameter the central vortex moves upstream the cavity. Also the velocity increases and volume fraction of non-Newtonian fluid after cavity increases. By increasing velocity, pressure decreases.

It is notable that, the changes in the velocity, pressure and volume fraction of fluids inside the channel and cavity are more sensible with changing the Reynolds number instead changing the rheological parameter, *n*.

Nomenclature

D – deformation tensor, [–]
f – the VOF function, [–]
H – channel height, [m]
n – rheological parameter, [–]

p – pressure, [Pa]
Re – Reynolds number, [–]
S – stress tensor, [–]
t – time, [s]
u, v – Cartesin velocities, [ms^{-1}]
u_{in} – inlet velocity, [ms^{-1}]
X, Y – Cartesian co-ordinates, [m]

Greek symbols

$\dot{\gamma}$ – shear rate, [s^{-1}]
λ – relaxation time, [s]
μ_0 – zero-shear-rate viscosity, [Pa·s]
μ_∞ – infinite-shear-rate viscosity, [Pa·s]
ρ – density, [kgm^{-3}]
τ_{xx},τ_{xy} – normal and shear stresses, [Pa]

References

[1] Taotao, F., *et al*., Flow Patterns of Liquid-Liquid Two-Phase Flow in Non-Newtonian Fluids in Rectangular Micro-Channels, Chemichal Engineering and Processing, *Process Intensification*, *91* (2015), May, pp. 114-120
[2] Achab, L., *et al*., Numerical Study of the Non-Newtonian Blood Flow in a Stenosed Artery Using Two Rheological Models, *Thermal Science*, *20* (2016), 2, pp. 449-460
[3] Demin, W., *et al*., Viscous-Elastic Polymer Can Increase in Cores, *Proceedings*, SPE Annual Technical Conference and Exhibition, Dalals, Tex., USA, 2000, pp. 2-8
[4] Huifen, X., *et al*., Elasticity of HPAM Solutions Increases Displacement Efficiency under Mixed Wettability Conditions, *Proceedings*, SPE Asia Pacific Oil and Gas Conference and Exhibition, Perth, Australia, 2004, pp. 18-20
[5] Huifen, X., *et al*., Experiment of Viscoelasticity of Polymer Solution (in Chinese), *Journal of Daqing Petroleum Institute*, (2002), 2, pp. 105-108
[6] Carreau, P. J., Rheological Equations from Molecular Network Theories, *Journal of Rheology*, *16* (1972), July, pp. 99-127
[7] Puyang, G., *et al*., Coupling of Finite Element Method and Discontinuous Galerkin Method to Simulate Viscoelastic Flows, *International Journal for Numerical Methods in Fluids*., *86* (2018), 6, pp. 414-432
[8] Bakhti, H., *et al*., Pulsatile Blood Flow in Constricted Tapered Artery Using a Variable-Order Fractional Oldroyd-B Model, *Thermal Science*, *21* (2016), 1A, pp. 29-40
[9] Huang, C., *et al*., An Improved KGF-SPH with a Novel Discrete Scheme of Laplacian Operator for Viscous Incompressible Fluid-Flows, *International Journal for Numerical Methods in Fluids*, *81* (2016), 6, pp. 377-396
[10] Xu, Y., *et al*., A Fractional Model for Time-Variant Non-Newtonian Flow, *Thermal Science*, *21* (2017), 1A, pp. 61-68
[11] Freydier, P., *et al*., Experimental Characterization of Velocity Fields Within the Front of Viscoplastic Surges Down an Incline, *Journal of Non-Newtonian Fluid Mechanics*, *240* (2017), Feb., pp. 56-69
[12] Dimitri, G., *Multi-Phase Flow and Fluidization*, Academic Press, San Diego, Cal., USA, 1994
[13] Autee, A., *et al*., An Experimental Study on Two-Phase Pressure Drop in Small Diameter Horizontal, Downward Inclind, and Vertical Tubes, *Thermal Science*, *19* (2015), 5, pp. 1791-1804
[14] Tsuji, Y., *et al*., Discrete Particle Simulation of 2-D Fluidized Bed, *Powder Technology*, *77* (1993), 1, pp. 79-87
[15] Zhou, L., *et al*., An SPH Pressure Correction Algorithm for Multi-Phase Flows with Large Density Ratio, *International Journal for Numerical Methods in Fluids*, *81* (2016), 12, pp. 765-788
[16] Boris, J. P., New Directions in Computational Fluid Dynamics, *Annual Review of Fluid Mechanics*, *21* (1989), pp. 345-385
[17] Sahil, O. U., Gretar, T., A Front-Tracking Method for Viscous, Incompressible, Multi-Fluid-Flows, *Journal of Computational Physics*, *100* (1992), 1, pp. 25-37
[18] Mazza, R. A., *et al*., Analyses of Liquid Film Models Applied to Horizontal and Near Horizontal Gas-Liquid Slug Flows, *Chemical Engineering Science*, *65* (2010), 12, pp. 3876-3892
[19] Jing-yu, X., *et al*., Study of Drag Reduction by Gas Injection for Power-Law Fluid-Flow in Horizontal Stratified and Slug Flow Regimes, *Chemical Engineering Journal*, *147* (2009), 2-3, pp. 235-244
[20] Jia, N., *et al*., Non-Newtonian Multi-Phase Flows: On Drag Reduction, Pressure Drop and Liquid Wall Friction Factor, *Chemical Engineering Science*, *66* (2011), 20, pp. 4742-4756
[21] Arun, A., *et al*., An Experimental Study on Two-Phase Pressure Drop in Small Diameter Horizontal, Downward Inclined and Vertical Tubes, *Thermal Science*, *19* (2015), 5, pp. 1791-1804
[22] Agus, S., *et al*., Two-Phase Flow Characteristics Across Sudden Contraction in Horizontal Rectangular Minichannel, *Journal of Mechanical Engineering and Automation*, *6* (2016), 3, pp. 58-64

[23] Patankar, S. V., *Numerical Heat Transfer and Flow*, McGraw-Hill, New York, USA, 1980
[24] Arakawa, C., *Computational Fluid Dynamics for Engineering*, University of Tokyo Press, Tokyo, Japan, 1994
[25] Ferziger, J. H., Peric, M., *Computational Methods for Fluid Dynamics*, Springer-Verlag, Berlin, Germany, 1996
[26] Bird, R. B., *et al*., *Dynamics of Polymeric Liquids*, Fluid Mechanics, John Wiley and Sons, Inc., New York, USA, 1977
[27] Giesekus, H., Dynamische und Thermodynamische Grundlagen, in: *Phanomenologische Rheologie*, Springer, New York, USA, 1994
[28] Hirt, C. W., Nichols, B. D., Volume of Fluid (VOF) Method for the Dynamics of Free Boundaries, *Journal of Computational Physics*, *39* (1981), 1, pp. 201-225
[29] Ruben, S., Stephane, Z., Direct Numerical Simulation of Free-Surface and Interfacial Flow, *Annu. Rev. Fluid Mech*., *31* (1999), pp. 567-603
[30] Min, S. K., Woo, I. L., A New VOF-Based Numerical Scheme for the Simulation of Fluid-Flow with Free Surface – Part I: New Free Surface-Tracking Algorithm and Its Verification, *International Journal for Numerical Methods in Fluids*, *42* (2003), 7, pp. 765-790
[31] Friedrich, G., *et al*., The 3-D CFD Simulation of Bottle Emptying Processes, *Journal of Food Engineering*, *109* (2012), 3, pp. 609-618
[32] Mustafa, T., Ferruh, E., Numerical Simulation for Heat Transfer and Velocity Field Characteristics of Two-Phase Flow Systems in Axially Rotating Horizontal Cans, *Journal of Food Engineering*, *111* (2012), 2, pp. 366-385
[33] Jeffrey, Y., *et al.*, Simulation of Slag-Skin Formation in Electroslag Remelting Using a Volume-of-Fluid Method, *Numerical Heat Transfer*, *67* (2015), 3, pp. 268-292
[34] Saincher, S., Banerjee, J., A Redistribution-Based Volume-Preserving PLIC-VOF Technique, *Numerical Heat Transfer*, *67* (2015), 4, pp. 338-362
[35] Takuya, Y., *et al.*, Validation of the S-CLSVOF Method with the Density-Scaled Balanced Continuum Surface Force Model in Multi-Phase Systems Coupled with Thermocapillary Flows, *International Journal for Numerical Methods in Fluids*, *83* (2017), 3, pp. 223-244
[36] Tome, M. F., *et al.*, A Finite Difference Technique for Simulating Unsteady Viscoelastic Free Surface Flows, *Journal Non-Newton. Fluid Mech*., *106* (2002), 2-3, pp. 61-106
[37] Darwish, M. S., Whiteman, J. R., Numerical Modelling of Viscoelastic Liquids Using a Finite-Volume Method, *Journal of Non-Newtonian Fluid Mechanics*, *45* (1992), 3, pp. 311-337
[38] Raanan, F., Raz, K., Time Dependent Simulation of Viscoelastic Flows at High Weissenberg Number Using the Log-Conformation Representation, *Journal of Non-Newtonian Fluid Mechanics*, *126* (2005), 1, pp. 23-37
[39] Ahmadi, M., Natural Convective Heat Transfer in a Porous Medium within a Two Dimension Enclosure, *IIUM Engineer Journal*, *18* (2017), 2, pp. 196-211
[40] Bram, V. L., Towards the Ultimate Conservative Difference Scheme: Monotonicity and Conservation Combined in a Second Order Scheme, *Journal of Computational Physics*, *14* (1974), 4, pp. 361-370
[41] Doormal, J. P. V., Raithby, G. D., Enhancement of the Simple Method for Predicting Incompressible Flows, *Numerical Heat Transfer*, *7* (1984), 2, pp. 147-163
[42] Skelland, A. H. P., Non-Newtonian Flow Heat transfer, John Wiley and Sons, New York, USA, 1967

Paper submitted: January 2, 2018
Paper revised: May 1, 2018
Paper accepted: May 6, 2018

© 2020 Society of Thermal Engineers of Serbia
Published by the Vinča Institute of Nuclear Sciences, Belgrade, Serbia.
This is an open access article distributed under the CC BY-NC-ND 4.0 terms and conditions